SATHISH CH[1*],
CHIDAMBARAM
IA[2],
MANIKANDAN
M[3]

JES

Journal of Electrical Systems

Switched Z-Source Boost Converter in Hybrid Renewable Energy System for Grid-Tied Applications

The world s focus is shifting toward Renewable Energy Sources (RES) as a result of the sharp rise in energy demand and the depletion of conventional energy sources. Distributed generation (DG) units developed on RES are easily and reliably integrated into grid due to microgrid technology. Inverters are typically used to integrate DGs into microgrid. At present, the fastest-growing renewable sources of electricity in the world is photovoltaic (PV) and wind energy conversion system (WECS), which evolved in response to growing environmental concerns about the risks of climate change connected with power generation. Recent technological developments have made it a top priority for researchers to find ways to enhance the efficiency of hybrid systems and the power converter stage. In order to achieve transmission losses and ensure energy savings, a new 13-bus system is developed in this work for regulating the output voltage in distribution networks. Switched Z-source Boost converter along with Proportional Integral (PI) controller is employed to boost the voltage obtained from PV system. A battery converter along with a bi-directional battery is connected to the DC link, to store energy generated by Hybrid Renewable Energy System (HRES) in excess amount. The obtained DC link voltage is transferred to three-phase voltage source inverter (VSI) for the conversion of DC to AC voltage. Effective harmonic reduction is attained with the aid of LC filter coupled to Three phase grid, and the PI controller associated to the grid supports in achieving effective grid synchronization. The proposed research is validated using MATLAB Simulink by considering the 13-bus system and an efficiency of 96.8 % is obtained with 0.93% Total Harmonic Distortion (THD).

Keywords: DG units, PV system, WECS, 13 bus system, Switched Z-source Boost Converter, Network Configuration.

1. Introduction

Energy supply and utilization challenges are associated with environmental issues like air pollution, acid rain, depletion of ozone layer, deforestation, and radioactive emissions in addition to global warming [1]. Potential countermeasures include reducing the usage of fossil fuels, increasing the availability of ecologically acceptable energy sources, and improving energy efficiency to conserve energy [2]. To combat an energy problem and environmental degradation, it is crucial to produce RES. Energy Storage Systems (ESS) offer flexibility to lessen the effects of RE access to grid because RE sources exhibit exceptional features of variable and uncertainty [3-5]. One of the biggest difficulties for researchers and engineers today is to generate energy from sources that are clean, efficient, and globally benign. Solar and wind energy are the two most promising RES for producing electricity with potential to make a sizable contribution to the world's electrical Energy needs. Both of these resources are nearly limitless, totally free, and emit no harmful by products or greenhouse gases [6]. But there is a certain amount of unpredictability with solar and wind energy because they are weather-dependent sources. While the generation of solar energy is generally predictable, that of wind energy is

[1*] Corresponding author: Sathish Ch, Research Scholar, Department of Electrical Engineering, Annamalai University, Tamilnadu, India, E-mail: anusmin2@gmail.com .

[2] Professor, Department of Electrical Engineering, Annamalai University, E-mail: driacdm@gmail.com.

[3] Professor, Department of Electrical Engineering, Jyothismathi Institute of science and Technology, E-mail: cm.manikandan@gmail.com.

sporadic, unreliable, and very unpredictable [7]. In this proposed work, hybrid power generation like Solar Photovoltaic [8] and WECS [9] has outperformed all other renewable energy sources due to a number of factors, including its availability in nature, environmental friendliness, minimal maintenance costs, and dependability. From an environmental standpoint, the primary goal of proposed study is to emphasize on green energy by reducing the use of energy derived from fossil fuels for the distribution system. According to several research studies in RES, the intermittent nature of photovoltaic sources necessitates the operation of converters to increase the voltage supplied from them. Typically DC-DC converters are employed to regulate power generation and to maximise electricity in varying climatic and environmental circumstances [10, 11]. In applications of photovoltaic system, Boost converters [12] are frequently employed for DC-DC conversion, however only step-up voltage ratios are feasible. The typical Buck-Boost converter [13], converts voltage in both step-up and step-down directions, but due to its interrupted input current, it cannot operate at its best without significant decoupling capacitors. Although Cuk [14] converter is capable of stepping voltage up or down it seems to have constant input currents. The enormous input power ripples still limits the performance of photovoltaic system under variable power points. Ideally, a massive PV array is required to possess accessibility and to track maximum power point of each of its individual panels to maximise power generation. The benefits of DC-DC Z-source [15] converters over traditional boost converters make them a great option for many applications involving renewable energies. However, since numerous discrete DC-DC converters must be employed, this is unworkable. To solve this problem, a Switched Z-Source driven DC-DC Boost converter is built, which uses fewer switches and is more efficient and reduces power losses. A RES like a solar photovoltaic system and battery power storage system is combined with the suggested structure. Efficient control techniques are necessary for a converter, in order to attain reduced settling time, steady state error, peak overshoot and to mitigate harmonics. In the proposed work, PI controller [16] is employed, which is simple conventional control approach to control DC voltages along with MPSO optimization strategy. Distributed generation (DG) is a crucial component of contemporary power networks, which also include energy storage technologies, RES, and load types like electric vehicles etc. [17]. The placement of the DGs ensures that they complement one another and maintain the microgrid's seamless operation. To assure improved operation of a microgrid in a grid-connected system, the control schemes within a module is created [18, 19]. In order to thoroughly investigate power quality disturbances and operating issues connected to the integration of RES into a balanced distribution network, this paper makes use of a standard IEEE 13-bus power system [20].

A hybrid approach consisting of PV/WECS/Battery is proposed in this article. The non-linear voltage obtained from PV system is improved with the utilization of Switched Z-source boost converter, which provides isolation by stepping up the voltage. For efficient control of the converter, the MPSO-PI controller is employed, which provides optimal result with its simple design. Similarly, the DFIG-based WECS associated to the proposed work generates AC voltage. In order to provide supply for DC bus, the PWM rectifier coupled to the WECS converts the AC voltage to DC. The generated DC supply from both sources is transferred to the DC link. The battery converter combined with the battery system collects the excess energy produced by the RES for later usage. The 3ϕ VSI provided converts DC voltage to AC, from which the voltage is supplied to LC filter for harmonics mitigation and supplied effectively to the grid. An IEEE 13 bus system is employed in this architecture to obtain equal amount of real and active power to the system by eliminating losses. The performance of the hybrid approach for the distribution system is validated using MATLAB simulation and improved results are obtained.

2. Proposed system

The growing demand for energy, combined with global concern for the environment and ongoing advancements in green technologies are creating new market prospects for renewable sources of energy. In order to reduce greenhouse gas emissions related to the production of electricity, RES like solar PV and WECS are used. A remarkable quick increase in low voltage distribution network and installations has been achieved through supportive regulations and incentives. Excessive voltage rise is brought on by bidirectional active power flow in Distribution Networks (DNs) to the grid. In the proposed work as shown in Figure 1, an efficient IEEE 13 bus distribution system is demonstrated for equal distribution of electricity to more number of supplies.
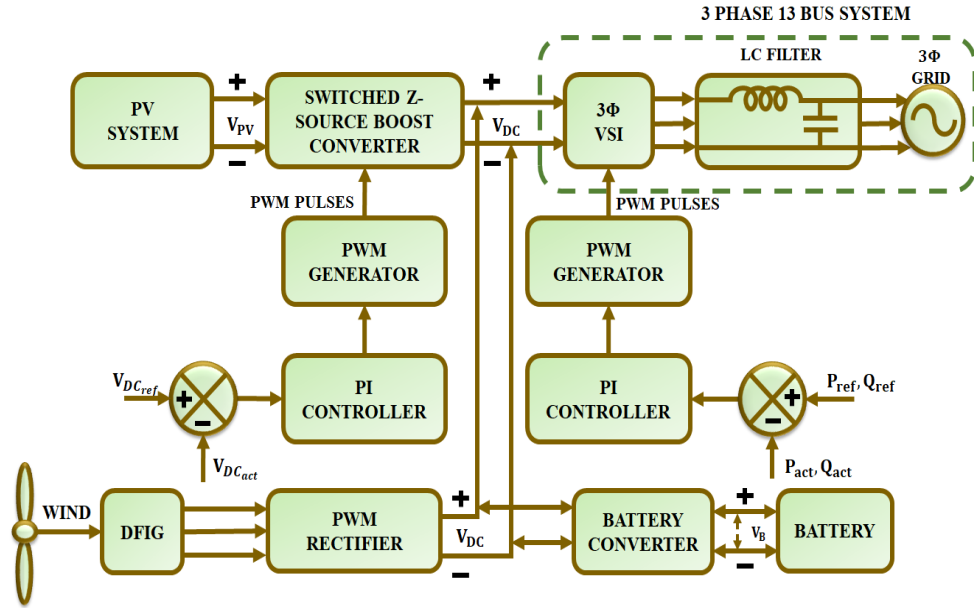

Fig. 1. Block Diagram of Proposed System

A HRES consisting of solar PV and WECS is proposed in this research for generating electricity by natural means. However, the intermittent nature affects the system performance. In order to enhance the voltage obtained from PV system, a converter approach is necessary. Usually DC-DC converter is employed to boost the voltage generated by PV system. In this proposed work Switched Z-source Boost converter is implemented, which is an advance form of boost converter. Consequently, PI controller is provided to control the converter voltage. Similarly, DFIG-WECS is the other RES for generating energy, which produces AC voltage. The acquired AC voltage is converted into DC with the aid of PWM rectifier. The acquired DC voltage is fed to DC link, from which the voltage is again transformed into AC, with the utilization of 3ϕ VSI. A bidirectional battery along with converter is placed in the DC link to acquire the excess energy generated and for utilization during intermittent condition. Thus, the 3ϕ VSI connected to grid via LC filter results in effective harmonic mitigation. The 3ϕ IEEE 13 bus system provided in the proposed work reduces the unbalanced distribution and provides equal power supply to different loads.

.
2.1. PV Modelling

A PV system is made up of cells arranged in an array which is either stationary or moved by motors in order to monitor the sun and maximise the amount of power produced. In addition to their high initial cost, one of the drawbacks of PV systems is that they require a lot of room to generate enough power. PV systems were initially utilised for massive corporations with extensive networks, but they now it is used for household and commercial uses.
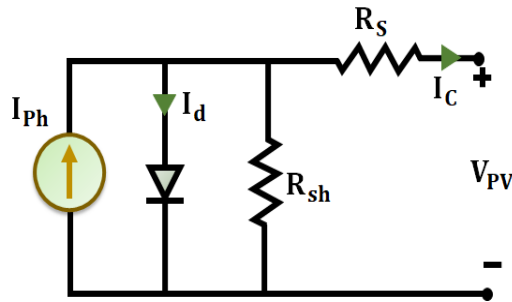

Fig. 2. Equivalent Circuit of Solar PV System

Multiple PV cells are connected in series and parallel in a photovoltaic solar system arrangement to provide the desired voltage. The circuit topology of the equivalent PV system is illustrated in Figure 2. According to semi-conducteur theory, the mathematical equation for I-V characteristics of a photovoltaic cell is expressed as,

$$I = I_{pv,cell} - I_{0,cell}\left[\exp\left(\frac{qv}{\alpha kT}\right) - 1\right] \tag{1}$$

Here, the Boltzmann constant is specified as K, electric charge as q, operating temperature as T.
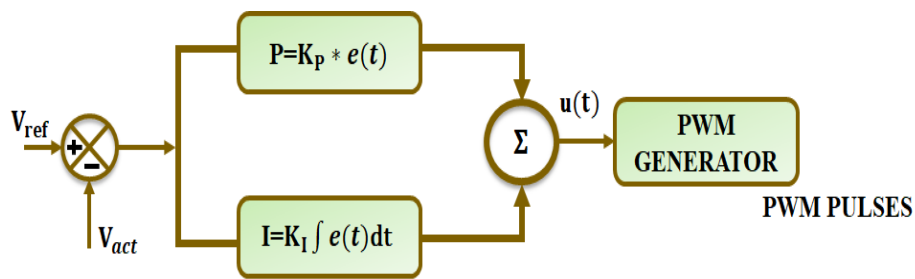
2.2. Proportional Integral Controller

Fig. 3. Schematic Representation of PI Controller

In practical applications, the PI controller is one of the most often utilised controllers. There are two tuning parameters for PI controllers, as shown in Figure 3. The proportional section and integral section make up both of its components. Here, deviations in steady

state error is caused by the proportional part, simultaneously the integral part removes the steady state error. The mismatch among a measured process parameter and the set reference point is used by a PI controller to determine an error value.

The output $u(t)$ specifies the PI Controller at time domain and is calculated as,

$$u(t) = k_p \, \mathrm{e}(t) + \mathrm{k_1} \int e(t)dt \qquad (2)$$

Here, error is denoted as $\mathrm{e}(t)$, Proportional gain as k_p and $\mathrm{k_1}$ specifies the integral gain factor evaluated from,

$$k_1 = \frac{k_p}{T_i} \qquad (3)$$

Here, reset time is represented as. T_i. Substituting Equation (3) in (2) the corresponding expression become

$$u(t) = k_p \, \mathrm{e}(t) + \frac{k_p}{T_i} \int e(t)dt \qquad (4)$$

2.3. Modelling of DFIG system

The main components of a DFIG-based WECS are Wind turbine, gearbox, wound-rotor induction machine, and a back-to-back converter. A typical representation of DFIG-based WECS is shown in Figure 4.Wind speed has a direct connection with kinetic power, which is calculated as follows:

$$P_a = \frac{1}{2} \rho S C_P(\lambda, \beta) V^3 \qquad (5)$$

Here, wind speed is specified as V, air density as ρ with value 1.225 kg/m^3 area surrounded by turbine blades as S and power conversion efficiency as C_P Subsequently, the aerodynamic torque T_a is expressed as,

$$T_a = \frac{p_a}{\Omega_t} = \frac{1}{2\Omega_t} \rho S C_P(\lambda, \beta) V^3 \qquad (6)$$

Where, turbine speed is represented as Ω_t.

A winding rotor asynchronous generator known as DFIG connects the grid directly to stator and rotor to the converter. The DFIG dynamic model utilized in this work is expressed in an arbitrary rotating frame for simplicity's sake. The voltage equations of stator and rotor is expressed as,

$$\begin{cases} v_{ds} = R_S i_{ds} + \dfrac{d}{dt}\phi_{ds} - \omega_s \phi_{qs} \\[2mm] v_{qs} = R_S i_{qs} + \dfrac{d}{dt}\phi_{ds} - \omega_s \phi_{ds} \\[2mm] v_{dr} = R_r i_{dr} + \dfrac{d}{dt}\phi_{dr} - \omega_r \phi_{qr} \\[2mm] v_{qs} = R_r i_{qr} + \dfrac{d}{dt}\phi_{qr} - \omega_r \phi_{dr} \end{cases} \tag{7}$$
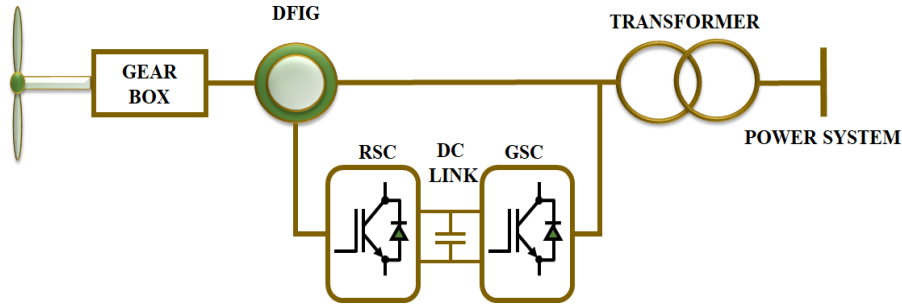

Fig. 4 Configuration of DFIG-WECS

Here, the stator and rotor indices is denoted as S and r, synchronous reference components as d and q, the flux, current and voltage is specified as ϕ, v and i and resistance as R.Similarly, the flux equations for stator and rotor is given by,

$$\begin{cases} \phi_{ds} = L_S i_{ds} + M i_{dr} \\[1mm] \phi_{qs} = L_S i_{qs} + M i_{qr} \\[1mm] \phi_{dr} = L_r i_{dr} + M i_{ds} \\[1mm] \phi_{qr} = L_r i_{qr} + M i_{qs} \end{cases} \tag{8}$$

This specifies inductance as L and mutual inductance as M.
For a DFIG-WECS the mechanical equation is expressed as,

$$J \frac{d\Omega}{dt} = T_a - T_{em} - f\Omega \tag{9}$$

Here, total inertia of turbine is denoted as J, DFIG speed as Ω, generator Electro Magnetic (EM) torque as T_{em} and damping co-efficient as f. The EM torque equation of DFIG is given by,

$$T_{em} = \rho \frac{M}{L_S}\left(\phi_{qs} i_{dr} - \phi_{ds} i_{qr}\right) \tag{10}$$

In which the number of pairs of poles in DFIG is represented as ρ.The corresponding active and reactive power at stator side is evaluated as,

$$\begin{cases} P_S = \dfrac{3}{2}(v_{ds}i_{ds} + v_{qs}i_{qs}) \\ Q_S = \dfrac{3}{2}(v_{qs}i_{ds} - v_{ds}i_{qs}) \end{cases} \qquad (11)$$

2.4. Switched Z-Source Boost Converter

An innovative Switched Z-source based boost converter is proposed, including strong step-up capability and minimal device voltage stress. The projected method provides input and output through a common ground that makes it more appropriate for specific applications. Figure 5 illustrates the equivalent circuit of proposed Switched Z- Source Boost converter.
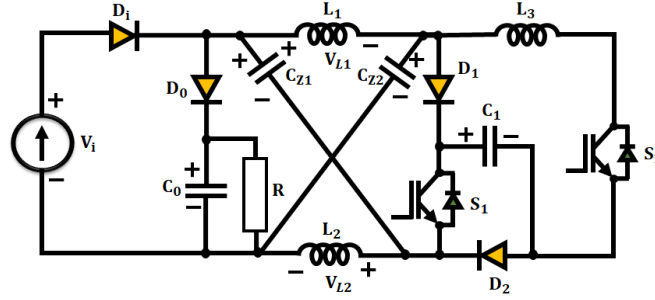
Fig. 5. Equivalent Circuit Topology of Proposed Converter

The topology of proposed Converter constitutes of a switched capacitor cell, and a Z-source network. The identical drive signal concurrently controls switches S_1 and S_2. The suggested converter also includes a capacitaire C_0, an output diode D_0, and an input diode D_i . .

Operating Modes of Proposed Converter :

This section compares and contrasts the Discontinuous Conduction Mode (DCM) and Continuous Conduction Mode (CCM) operating philosophies. The following analysis makes the following presumptions.

- The capacitors are all of an adequate size. As a result, capacitors' voltage is conceived as constant for a switching period.
- The power equipment is perfect, and the parasitic components are ignored.

Inductors L $_1$ and L $_2$ have same level of inductance due to similarity of the topologies.

a) Operation at CCM

Mode $1[t_0 - t_1]$: Switches S_1, S_2 and output diode D_0 are in ON state, and the diodes D_1, D_2 and D_i are reversed biased using $V_0 - V_i$ and V_{C1}. The current flow is indicated in Figure 6(a). The inductor L_1 is charged via capacitor C_{Z1} and C_1, while the

other inductor L_2 is charged by C_{Z2} and C_2 capacitors. In the interim, C_{Z1}, C_{Z2} and C_1 are linked in series to charge loads R and C_0. Equations (12) and (13) are acquired, in accordance with Kirchhoff Voltage Law (KVL).

$$\begin{cases} V_{L1} = V_{C1} + V_{CZ1} \\ V_{L2} = V_{C1} + V_{CZ2} \end{cases} \tag{12}$$

$$V_0 = V_{C1} + V_{CZ1} + V_{CZ2} \tag{13}$$

Mode 2: $[t_1 - t_2]$: Diodes D_1, D_2 and D_i are turned ON and switches are turned OFF. The output diode D_0 is reversed biased by $V_0 - V_i$. The direction of current flow is represented in Figure 6(b). The capacitor of converter V_{CZ1} is charged by V_i and V_{CZ2} using V_i and L_1. The capacitor C_1 is charged additionally, by inductors L_1, L_2 and V_i. C_0 Is responsible for sustaining the output voltage. These connections are made, according to KVL.

$$\begin{cases} V_{L1} = V_{C1} + V_{CZ1} \\ V_{L2} = V_{C1} + V_{CZ2} \\ \quad V_{L3} - V_{C1} \end{cases} \tag{14}$$

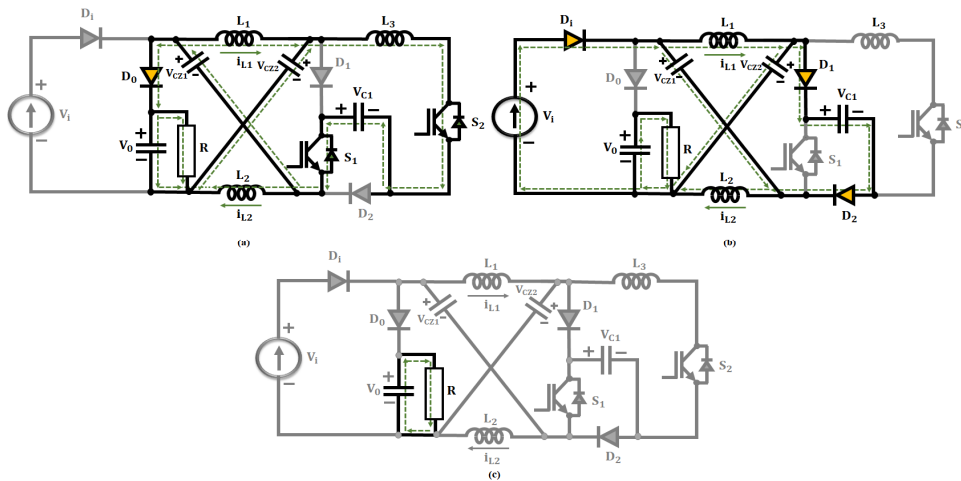$$V_{C1} = V_{CZ1} + V_{CZ2} - V_i \tag{15}$$

Fig. 6. Direction of Current Flow during (a) Mode1 at CCM &DCM, (b) Mode 2 at CCM &DCM and (c) Mode 3 at DCM

   b)   Operation at DCM

In DCM mode 3 Operating Modes are there and the corresponding timing waveform is depicted in Figure 7.

71

Mode 1 $[t_0 - t_1]$: The circuit topology is same as that of in CCM and Equations (12) and (13) are still applicable at this stage. Considering $L_1 = L_2 = L$, the fluctuation of inductor current throughout this time period can be estimated as follows,

$$\begin{cases} \Delta i_{L1} = \dfrac{(V_{CZ1} + V_{C1})}{L} D T_S \\[3mm] \Delta i_{L2} = \dfrac{(V_{CZ2} + V_{C2})}{L} D T_S \end{cases} \qquad (16)$$

Mode 2 $[t_1 - t_2]$ the direction of current flow is same as that of operation in continuous conduction mode. Similarly, the Equations (14) and (15) of CCM mode exists. The operation of mode 2 terminates whenever the inductor current at time t_2 falls to zero.

Mode 3 $[t_2 - t_3]$: At this instance all diodes and switches are in OFF state and the voltage at output is maintained with C_0 . The equivalent circuit topology corresponding to this mode is illustrated in Figure 6(c). Mode 3 terminates when the switches are at ON state at time t_3 , which is the beginning of subsequent switching period.
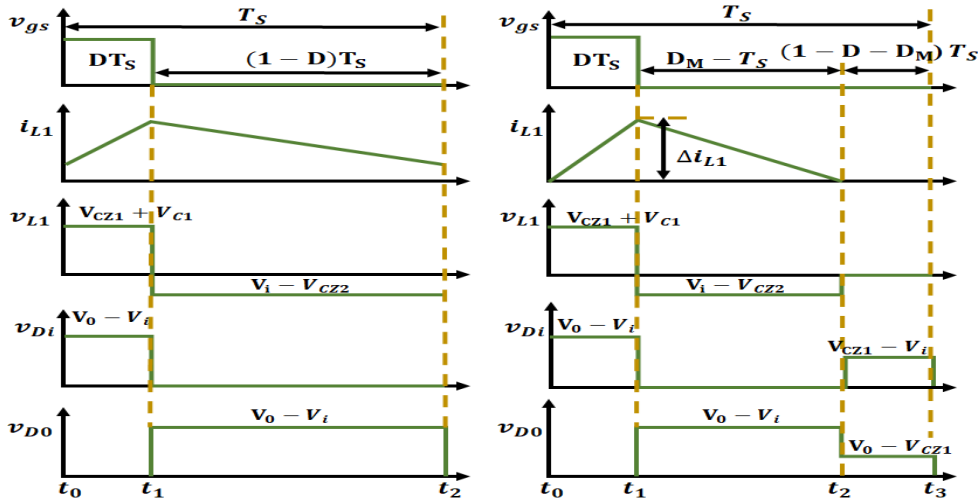

Fig. 7. Waveform of Proposed Converter at CCM and DCM Mode

2.5. Modelling of IEEE 13 Bus System

This suggested work makes use of IEEE 13 bus distribution system, which runs at 4.16 kV, has asymmetrical loading, is quite short, and is heavily loaded. In addition, this circuit has a single in-line transformer, overhead and underground wires, shunt capacitors, and a single voltage regulator at the substation. In Figure 8, the proposed topology is illustrated. There are buses with 1, 2, and 3 phases in this IEEE 13 bus system. It has 32 nodes in total. It is expected that each of the 32-circuit nodes has a metre that measures the voltage magnitude. As a result of closed switch connecting buses 671 and 692, the voltage magnitude of their phases is the same. The load time profiles are same for all of the loads.

Load Model :

The 13 bus test feeder is a significantly loaded system made up of 3ϕ and 1ϕ loads coupled in delta or Y topology with constant PQ, I, or Z. Simulink's dynamic load block is used to represent 3ϕ balanced loads, while 1ϕ dynamic load blocks are used to describe the unbalanced loads. Given equations (17) and (18) are the actual power P and reactive power Q for load.

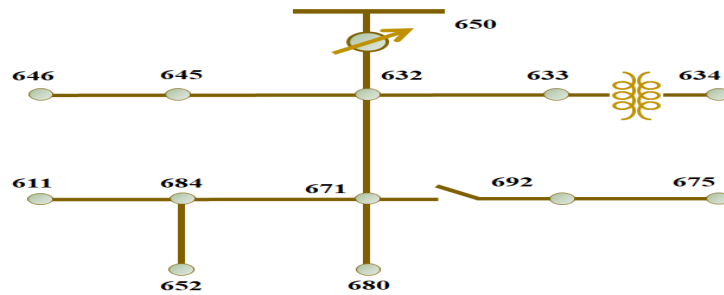$$P = P_0 \left(\frac{V}{V_0} \right)^{np} \tag{17}$$

$$Q = Q_0 \left(\frac{V}{V_0} \right)^{nq} \tag{18}$$

Fig. 8. Configuration of IEEE-13 Bus System

Here, the initial values of voltages, active and reactive power is indicated by V_0, P_0 and Q_0. The constants np and nq regulate the load's PQ, I, or Z type.

3. Results and Discussion

The proposed approach consisting of PV, WECS along with battery for steady power studied in this work. The adoption of Switched Z-source boost converter along with PI controller results in stabilized PV voltage. The performance of proposed work based on IEEE 13 bus distribution system is analyzed using MATLAB simulation and the validated results obtained are as follows. Table 1 specifies the parameter specification of Solar, Wind and Battery

Table 1:   Spécifications of Solar PV System, WECS and BESS

Parameters	Specifications
Solar PV Panel	
Peak Power	10kw
No. of Solar PV Panels	750w,13panels
Short Circuit Voltage	12v
Open Circuit Current	22.6 A

Short Circuit Voltage	62.5A
No. of Series Connected Solar Cells	36
WECS	
No. of Wind Turbines	1
Power	10kw
Voltage	575v
Speed Range	4m/s-16m/s
Switched Z-Source Boost Converter	
Cz_1, cz_2	22 μ F
C_0, C_1	1000 μ F
L_1, L_2	4mH
Battery Converter	
L	1mH
C	1000 μ F
Switching Frequency	10KHZ
Load	
Capacity	5KW

The waveforms obtained from MATLAB Simulink for the proposed approach are as follows:
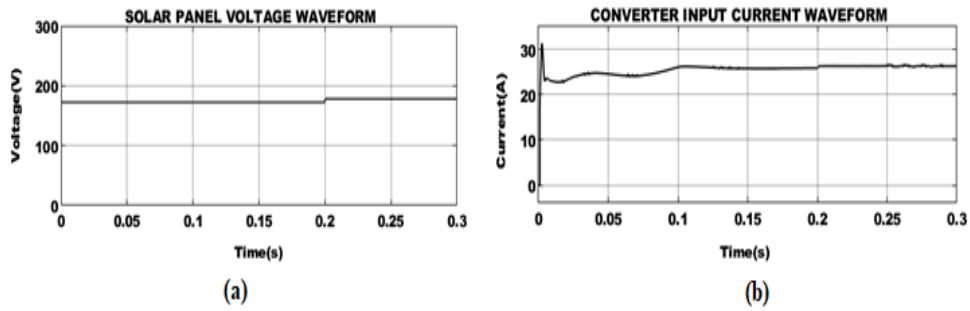
Fig.9.Solar Panel Output of (a) Voltage and (b) Current

The voltage and current obtained from Solar PV is illustrated in the waveform, shown in Figure 9. It is observed that, the input voltage of solar PV is maintained constant after 0.2S while the output current 25A is obtained constant after 0.1s. Corresponding to solar PV outputs at variable operating conditions cause's changes in the converter output
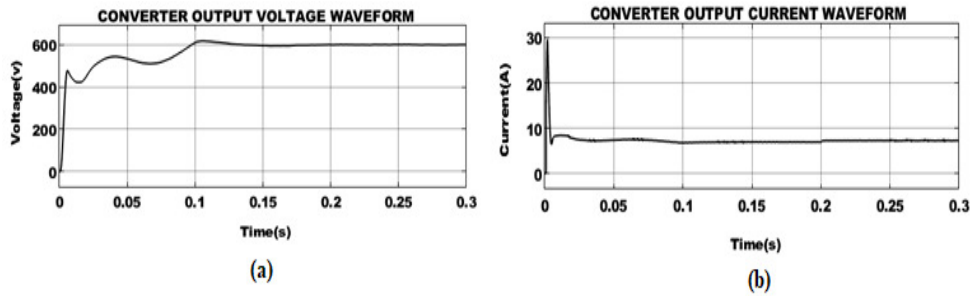
Fig. 10 : Switched Z-Source Converter (a) Output Voltage and (b) Output Current

The proposed converter's output voltage and current waveform is shown Figure 10. It is noticed that, the output voltage of converter initially increases with respect to times and fluctuates till 0.1s.A constant voltage of 600V is obtained after 0.1S with the aid of conventional PI controller employed. Similarly, the output current reaches a peak value of 30A and maintained constant after 0.15S with 8A current. Thus, the proposed controller approach results in generating improved voltage and current
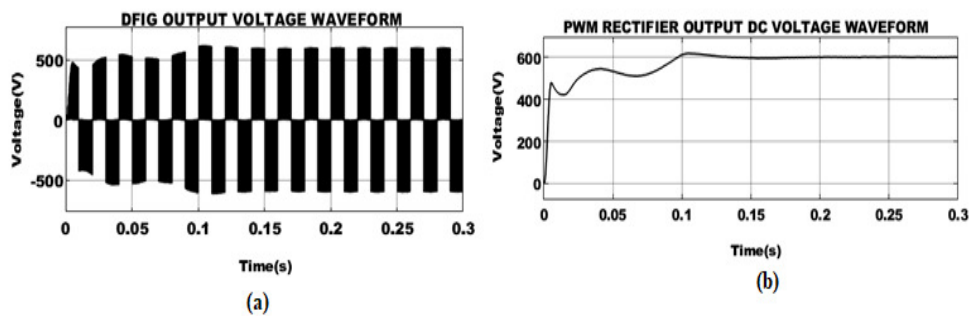

Fig 11 : Output Voltage Waveform for (a) DFIG –WECS and (b) PWM Rectifier

Owing to intermittent nature of Wind system a constant voltage of 550V is obtained after 0.1S is depicted in Figure11 (a). Subsequently, after a sudden rise in voltage at 0.02S the converted DC voltage using PWM rectifier achieves a maximum voltage of 600V at 0.1S and is further maintained constant as shown in Figure 11(b).
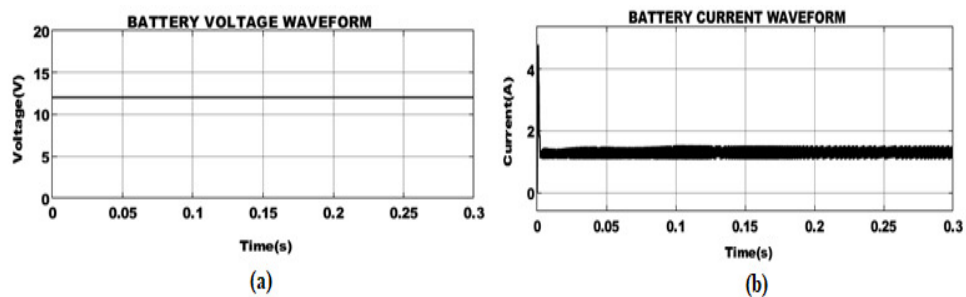

Fig. 12. Battery (a) Voltage and (b) Current Waveform

Figure 12 represents voltage waveform and current waveform of battery, in which the battery voltage is maintained as a constant of 12V and the corresponding battery current is subjected to minor fluctuations and maintained stable within a short time period.
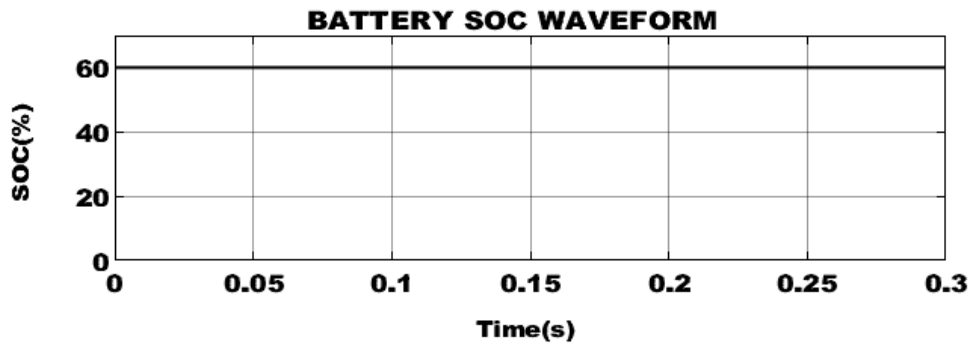

Fig.13. SOC of Battery

The SOC of the bidirectional battery implemented in this work with 60%charge is depicted in Figure 13. Here, the battery operates in buck mode when it is below 60%. At that instance the battery starts charging. While boost operation is performed, when the SOC of battery is above 60%, during this occasion the battery discharges
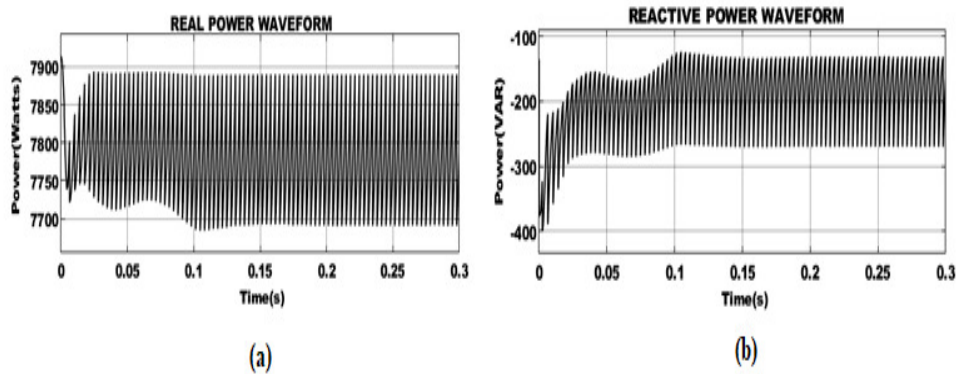

Fig. 14: (a) Real and (b) ReactivePower Waveforms.

The implementationof 13 bus distribution system results in maintaining a constant real and reactive power is illustrated in Figure 14. From figure 14(a), it is observed that a stable real power of 7900W is obtained at 0.03S. Similarly, the corresponding reactive power of -150VARis attained after minor fluctuations as shown in Figure 14(b).

(a)   (b)
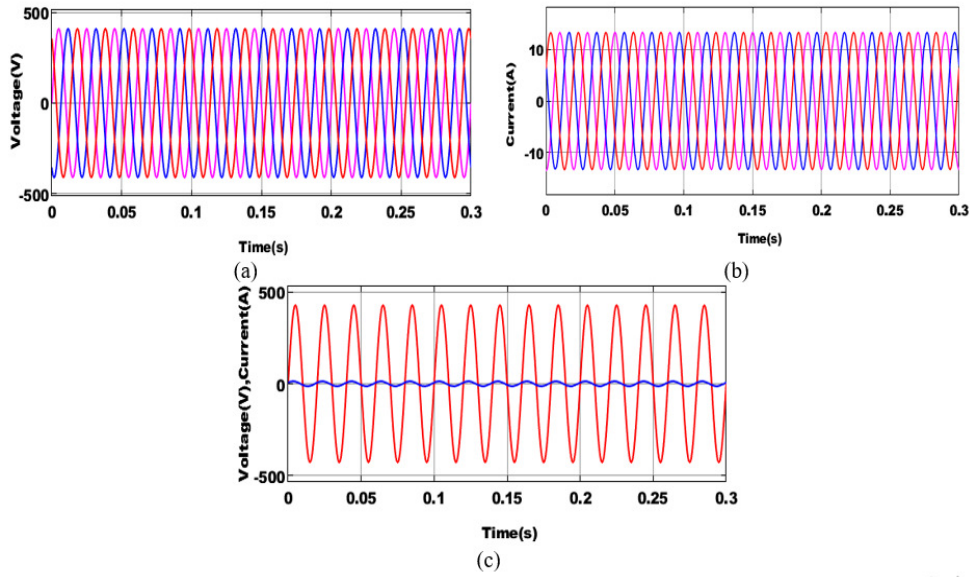

(c)

Fig. 15. Waveforms for (a) Grid Voltage (b) Grid Current and (c) Grid Voltage and Current

The waveform illustrated in Figure 15(a) indicates the Grid voltage without any fluctuations. Similarly fromFigure15(b)a stable grid current of 12A is Maintained. A combined waveform for grid voltage and current is depicted in Figure 15(c), in which a stable grid voltage of 450V and Grid current of 12A is maintained.
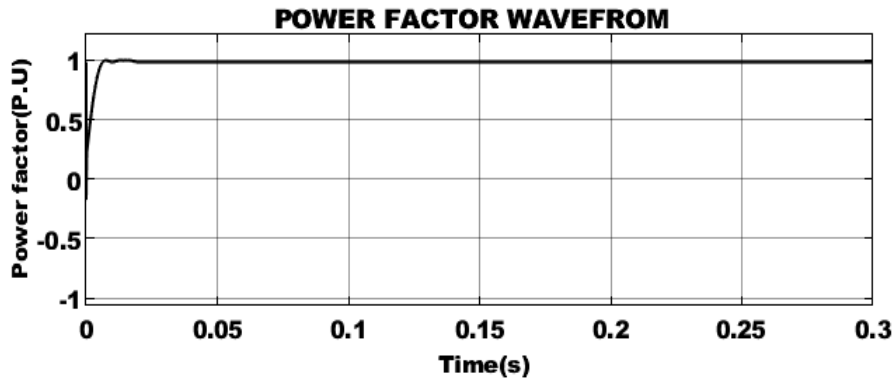

fig.16 : Power Factor Waveform

The power factor waveform for the proposed approach is illustrated in Figure 16. From the figure it is observed that, after 0.02s unity power factor is achieved

A comparative analysis is performed in terms of efficiency with other converter as shown in Table 2.

Table 2: Comparison of Proposed Converter with Existing System

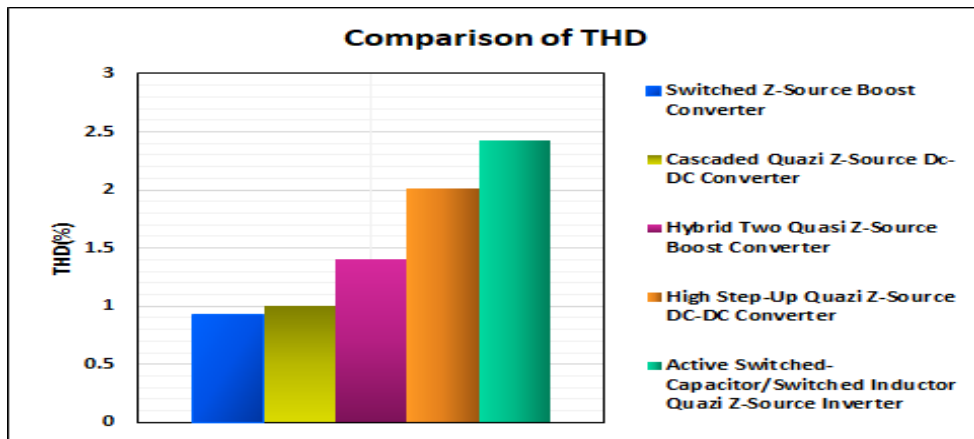| No. of Diodes	No. of Switches	No. of Inductors	No. of Capacitors	Voltage Gain	Efficiency (%)
4	2	2	4	$G = \dfrac{1-3D}{1-4D}$	96.8%
3	1	3	5	$G = \dfrac{1}{1-3D}$	95.6%
4	1	4	7	$G = \dfrac{1}{1-4D}$	95%
5	1	3	7	$G = \dfrac{2+D}{1-2D}$	94.7%
6	2	2	2	$G = \dfrac{1+D}{1-3D}$	94%

Fig 17. Comparison of THD

The comparsion of total harmonic distortion is depicted in Figure 17, in which the comparison is explored between various converters. The proposed converter with the support of PI controller attains a THD of 0.93%, which is minimum in contrast to other converters. Thus resulting in untiy power factor
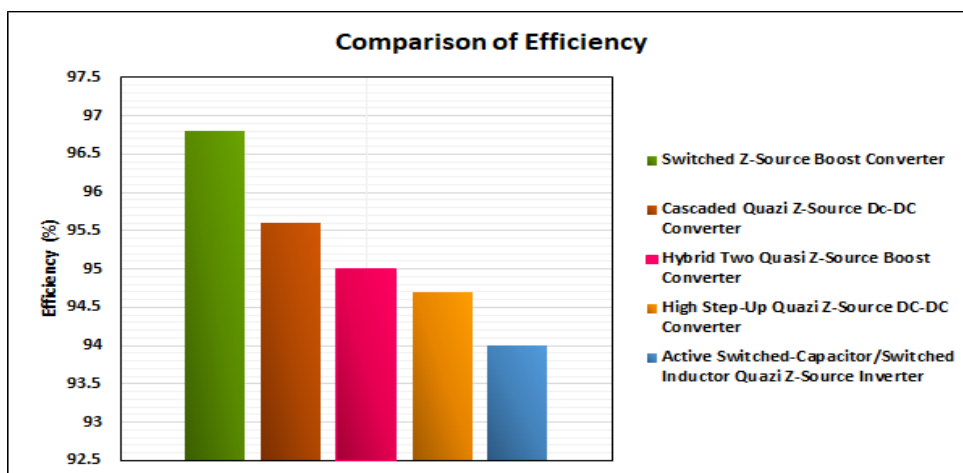
Fig.18. Comparison of Efficiency (%) with Existing converters

It is observed from Figure 18 that, proposed Switched Z-Source Boost converter attains better efficiency in comparison with existing DC-DC converter topologies. The efficiency of proposed converter with the assistance of PI Controller is 96.8%, which is higher in comparison with the other four converter approches.

4. Conclusion

As the world's energy needs are increasing and conventional energy sources are running out, and much attention is becoming paid to renewable energy sources. This is because of the sharp rise in energy costs. In this work, HRES combining PV and WECS system is implemented. This study makes a suggestion for an improved DC-DC converter that is ideally suited for photovoltaic applications that demand a high level of efficiency. The enhanced DC-DC converter is based on integration of Z-Source and Boost converters. The utilization of PI controller aids is providing stabilized voltage to the converter. The implemented 13 bus distribution network is simulated with 3ϕ system and the corresponding results are obtained using MATLAB Simulink. The comparative analysis is made among different converters in terms of efficiency, in which the proposed Switched Z-Source Boost converter achieves an improved efficiency of 96.8% with reduced harmonics of 0.93% and voltage gain of 1:12 respectively.

References

[1] K.S. Kavin, and P. Subha Karuvelam, "PV-based grid interactive PMBLDC electric vehicle with high gain interleaved DC-DC SEPIC Converter", IETE Journal of Research, pp.1-15, Aug2021.doi:10.1080/03772063.2021.1958070.

[2] P. K. Bonthagorla and S. Mikkili, "Performance Investigation of Hybrid and Conventional PV Array Configurations for Grid-connected/Standalone PV Systems," in CSEE Journal of Power and Energy Systems, vol. 8, no. 3, pp. 682-695,May 2022. Doi: 10.17775/CSEEJPES.2020.02510.

[3] M. I. Mosaad, H. S. M. Ramadan, M. Aljohani, M. F. El-Naggar and S. S. M. Ghoneim, "Near-Optimal PI Controllers of STATCOM for Efficient Hybrid Renewable Power System," in IEEE Access, vol. 9, pp. 34119-34130, 2021. Doi: 10.1109/ACCESS.2021.3058081.

[4] Z. Shi, W. Wang, Y. Huang, P. Li and L. Dong, "Simultaneous optimization of renewable energy and energy storage capacity with the hierarchical control," in CSEE Journal of Power and Energy Systems, vol. 8, no. 1, pp. 95-104, Jan. 2022, doi: 10.17775/CSEEJPES.2019.01470.

[5] F. Blaabjerg, Y. Yang, D. Yang and X. Wang, "Distributed Power-Generation Systems and Protection," in Proceedings of the IEEE, vol. 105, no. 7, pp. 1311-1331, July 2017, doi: 10.1109/JPROC.2017.2696878.

[6] V. Prema, M. S. Bhaskar, D. Almakhles, N. Gowtham and K. U. Rao, "Critical Review of Data, Models and Performance Metrics for Wind and Solar Power Forecast," in IEEE Access, vol. 10, pp. 667-688, 2022, doi: 10.1109/ACCESS.2021.3137419.

[7] Z. Wang et al., "Study on the Optimal Configuration of a Wind-Solar-Battery-Fuel Cell System Based on a Regional Power Supply," in IEEE Access, vol. 9, pp. 47056-47068, 2021. DOI: 10.1109/ACCESS.2021.3064888.

[8] M. Elkayam and A. Kuperman, "Optimized Design of Multiresonant AC Current Regulators for Single-Phase Grid-Connected Photovoltaic Inverters," in IEEE Journal of Photovoltaics, vol. 9, no. 6, pp. 1815-1818, Nov. 2019, doi: 10.1109/JPHOTOV.2019.2937386.

[9] S. Velpula, R. Thirumalaivasan and M. Janaki, "Stability Analysis on Torsional Interactions of Turbine-Generator Connected With DFIG-WECS Using Admittance Model," in IEEE Transactions on Power Systems, vol. 35, no. 6, pp. 4745-4755,Nov.2020, doi: 10.1109/TPWRS.2020.2992111.

[10] J. Zhao and D. Chen, "Switched-Capacitor High Voltage Gain Z-Source Converter With Common Ground and Reduced Passive Component," in IEEE Access, vol. 9, pp. 21395-21407,2021, doi: 10.1109/ACCESS.2021.

[11] K. Nathan, S. Ghosh, Y. Siwakoti and T. Long, "A New DC–DC Converter for Photovoltaic Systems: Coupled-Inductors Combined Cuk-SEPIC Converter," in IEEE Transactions on Energy Conversion, vol. 34, no. 1, pp. 191-201, March 2019, doi: 10.1109/TEC.2018.2876454

[12] R. Errouissi, A. Al-Durra and S. M. Muyeen, "A Robust Continuous-Time MPC of a DC–DC Boost Converter Interfaced With a Grid-Connected Photovoltaic System," in IEEE Journal of Photovoltaics, vol. 6, no. 6, pp. 1619-1629, Nov. 2016, doi: 10.1109/JPHOTOV.2016.2598271.

[13] S. Siouane, S. Jovanović and P. Poure, "Open-Switch Fault-Tolerant Operation of a Two-Stage Buck/Buck–Boost Converter With Redundant Synchronous Switch for PV Systems," in IEEE Transactions on Industrial Electronics, vol. 66, no. 5, pp. 3938-3947, May 2019, doi: 10.1109/TIE.2018.2847653.

[14] J. C. d. S. de Morais, J. L. d. S. de Morais and R. Gules, "Photovoltaic AC Module Based on a Cuk Converter With a Switched-Inductor Structure," in IEEE Transactions on Industrial Electronics, vol. 66, no. 5, pp. 3881-3890, May 2019, doi: 10.1109/TIE.2018.2856202.

[15] Babu V., Ahmed K.S., Shuaib Y.M., Manikandan M.(2021) Power Quality Enhancement Using Dynamic Voltage Restorer (DVR)-Based Predictive Space Vector Transformation PSVT) With Proportional Resonant (PR)-Controller. IEEE Access, 2021, vol. 9, pp. 155380-(155392. doi: https://doi.org/10.1109/ACCESS.2021.3129096

[16] J. Liu, J. Wu, J. Qiu and J. Zeng, "Switched Z-Source/Quasi-Z-Source DC-DC Converters With Reduced Passive Components for Photovoltaic Systems," in IEEE Access, vol. 7, pp. 40893-40903, 2019, doi: 10.1109/ACCESS.2019.2907300.

[17] K. Y. Ahmed, N. Z. Bin Yahaya, V. S. Asirvadam, N. Saad, R. Kannan and O. Ibrahim, "Development of Power Electronic Distribution Transformer Based on Adaptive PI Controller," in IEEE Access, vol. 6, pp. 44970-44980, 2018, doi: 10.1109/ACCESS.2018.2861420.

[18] M. Alshareef, Z. Lin, F. Li and F. Wang, "A grid interface current control strategy for DC microgrids," in CES Transactions on Electrical Machines and Systems, vol. 5, no. 3, pp. 249-256, Sept. 2021. DOI:10.30941/CESTEMS.2021.00028.

[19] B. Imtiaz, I. Zafar, and C. Yuanhui, "Modelling of an Optimized Micro grid Model by Integrating DG Distributed Generation Sources to IEEE 13 Bus System", European Journal of Electrical Engineering and Computer Science, vol.5, no.2, pp.18-25, 2021. https://doi.org/10.24018/ejece.2021.5.2.309.

[20] M. Farrokhabadi, S. König, C. A. Cañizares, K. Bhattacharya and T. Leibfried, "Battery Energy Storage System Models for Micro grid Stability Analysis and Dynamic Simulation," in IEEE Transactions on Power Systems, vol. 33, no. 2, pp. 2301-2312, March 2018, doi: 10.1109/TPWRS.2017.2740163.

[21] O. P. Mahela, B. Khan, H. H. Alhelou and P. Siano, "Power Quality Assessment and Event Detection in Distribution Network With Wind Energy Penetration Using Stockwell Transform and Fuzzy Clustering," in IEEE Transactions on Industrial Informatics, vol. 16, no. 11, pp. 6922-6932, Nov. 2020, doi: 10.1109/TII.2020.2971709.

[22] D. Vinnikov, I. Roasto, R. Strzelecki and M. Adamowicz, "Step-Up DC/DC Converters With Cascaded Quasi-Z-Source Network," in IEEE Transactions on Industrial Electronics, vol. 59, no. 10, pp. 3727-3736, Oct. 2012, doi: 10.1109/TIE.2011.2178211.

[23] H. Shen, B. Zhang and D. Qiu, "Hybrid Z-Source Boost DC–DC Converters," in IEEE Transactions on Industrial Electronics, vol. 64, no. 1, pp. 310-319, Jan. 2017, doi: 10.1109/TIE.2016.2607688.

[24] M. M. Haji-Esmaeili, E. Babaei and M. Sabahi, "High Step-Up Quasi-Z Source DC–DC Converter," in IEEE Transactions on Power Electronics, vol. 33, no. 12, pp. 10563-10571, Dec. 2018, doi: 10.1109/TPEL.2018.2810884.

[25] Babu V., Ahmed K.S., Shuaib Y.M., Mani M. (2021) A novel intrinsic space vector transformation based solar fed dynamic voltage restorer for power quality improvement in distribution system. Journal of Ambient Intelligence and Humanized Computing. doi: https://doi.org/10.1007/s12652-020-02831-0